Springer

KSME

Journal of Mechanical Science and Technology 33 (11) (2019) 5581~5588
www.springerlink.com/content/1738-494x(Print)/1976-3824(Online)
DOI 10.1007/s12206-019-1051-1

An experimental study of a spring-loaded needle-free injector: Influence of the ejection volume and injector orifice diameter †

Dongping Zeng[1,2,3], Ni Wu[1,2,3], Lu Xie[1,2,3], Xiaoxiao Xia[1,2,3] and Yong Kang[1,2,3,*]

[1]*School of Power and Mechanical Engineering, Wuhan University, Wuhan, China*
[2]*Hubei Key Laboratory of Accoutrement Technique in Fluid Machinery and Power Engineering, Wuhan University, Wuhan, China*
[3]*Hubei Key Laboratory of Waterjet Theory and New Technology, Wuhan University, Wuhan, China*

(Manuscript Received April 15, 2019; Revised July 2, 2019; Accepted September 3, 2019)

Abstract

Needle-free injection is an alternative strategy to conventional needle injection in the field of drug delivery. This approach offers a number of advantages, especially in reducing complaints of needle phobia and avoiding the occurrence of accidental needle stick injuries. The ejection volume and orifice diameter are inherently important in determining the injection depth and percent delivery. In this study, we investigate the dispersion pattern of liquid penetration into gels and porcine tissues using a needle-free injector with ejection volumes of 0.05 to 0.35 mL and orifice diameters of 0.17 to 0.50 mm. In addition, the influence of the two parameters is analyzed quantitatively on the dispersion pattern through impact experiments and injection experiments. Furthermore, an equation of the jet power calculated by the ejection volume and orifice diameter is proposed to describe the delivery fraction of the injection experiments. Controls of the ejection volume and orifice diameter are demonstrated to help achieve a more effective injection process and a better injection experience.

Keywords: Biomedical devices; Fluid dispersion; Jet penetration; Jet power; Needle-free injection; Transdermal drug delivery

1. Introduction

Needles and syringes are currently the leading method to deliver drugs subcutaneously. In addition, transdermal drug delivery plays an irreplaceable role in the delivery of biological macromolecules. However, needle injection is considered a low-compliance injection method since it is readily associated with needle cross-contamination and sharp injury [1-3]. This condition has prompted research on the development of alternative strategies for transdermal drug delivery. The first clinical trial of needle-free injection (NFI) was in the 1930s and it uncovered that the NFI was as effective as conventional needle injection for drug administration [2, 4]. The tested technology was able to puncture skin by a high-speed stream of fluid and deliver drugs to intradermal, subcutaneous and intramuscular tissues for animal and human immunization without needles. There are a number of different types of needle-free injectors that can be distinguished by their driving source, such as air-powered injection devices [5], Lorentz-force drivers [6, 7] and piezoelectric actuators [8]. Thus far, NFI has shown significant advantages over conventional injection methods for high injection completion rates and remarkable bioavailability. As a result, several macromolecule drugs, such as vaccines, insulin and growth hormones, have been administrated via NFI [9-11]. Although the NFI has obvious superiorities, there still exist many complaints about bruising and accidental bleeding, which lead to low patient acceptance of this injection method. To alleviate problems such as incomplete delivery of medication and excessive penetration, many studies have been conducted to improve injection performance.

Theoretical research was conducted by Baker and Sanders on spring-loaded needle-free injectors [12]. They pointed out that the design of the injector influences the injection performance and that the fluid pressure profile can be evaluated by the mathematical model. Additionally, some researchers have suggested that the nozzle geometry and jet shape affect the dispersion pattern of fluid penetration [13]. The reason is that a suitable dispersed jet shape with adjusted velocity is able to target a desired layer of tissue for clinical application. The performance of jet penetration into the skin from the spring-loaded NFI was mainly varied by two main injection parameters: The ejection volume and orifice diameter. The dependence of jet penetration into human skin on these parameters has been recently reported in the literature. It was reported that the time required to attain the peak jet velocity increased, whereas the peak jet velocity decreased, with increasing ejec-

*Corresponding author. Tel.: +86 27 68774442, Fax.: +86 27 68774442
E-mail address: Kangyong@whu.edu.cn
† Recommended by Associate Editor Won Hyoung Ryu

tion volume, which was due to the increase in the impact pressure at the nozzle exit [8, 14]. And the area of the dispersion region increased as the increasing injected volume in the vitro experiment for porcine skin [15]. Furthermore, the ejection volume has a direct influence on the injection duration in NFI [16]. For the orifice diameter of the injector, the injection depth drops sharply with increasing diameter [17, 18]. The reason is that the hydraulic loss increases sharply as the orifice diameter increases. Although these studies have revealed the effect of different injection parameters, there is still no quantitative description of the effect of the two different injection parameters on the dispersion pattern of jet penetration and only a brief statement of the experimental results. Furthermore, the combined influence of the ejection volume and orifice diameter on the injection efficiency is currently unclear. Therefore, a precise understanding of the impact of these parameters is a critical next step towards the effective clinical application of NFI.

In this work, we focus on the effect of the ejection volume and orifice diameter on the dispersion pattern of the liquid penetration in NFI. Impact experiments for the needle-free injector with different parameters are conducted in order to reveal how different injection parameters affect the impact pressure and the duration of injection. Then, quantitative analysis of the influence of different ejection volumes and orifice diameters on the diffusion pattern of liquid penetration into the soft material is conducted using injection experiments in gels and porcine tissues. Moreover, we propose an equation of the exit jet power associated with the ejection volume and orifice diameter with the aim of exploring the dependence of injection efficiency in gels as well as in porcine tissues on the ejection volume and orifice diameter.

2. Materials and method

2.1 Materials

SDS-polyacrylamide gel was used in the injection experiments since it has a similar Young's modulus to human epidermal tissue [8, 19, 20]. The mechanical properties of the gels were varied by simply changing the mass/volume percentage of acrylamide in each gel. In this study, gels (10 % acrylamide) were polymerized by adding initiators (10 % ammonium persulfate and N,N,N0,N0-tetramethylethylenediamine) to a 30 % (acr-bis) acrylamide solution of 29:1 acrylamide to bisacrylamide. SDS-polyacrylamide gel preparation kits were purchased from Beyotime Biotechnology Company (Jiangsu, China). Acrylamide solution (40 % [w/v]) was mixed with DI water to create solutions possessing various acrylamide concentrations in 10 % [w/v]. The volumes of DI water, 30 % (acr-bis) acrylamide solution, 10 % APS and 10 % SDS to prepare the 50 mL gel solution were 13.3, 16.7, 0.5 and 0.5 mL, respectively.

The penetration of porcine tissue has frequently been used in NFI studies to simulate the penetration of human dermal tissue owing to comparability of the thickness of the stratum corneum, the stiffness of tissues and the analogous jet speed in both ex vivo human and porcine tissue [6, 19, 21-24]. Postmortem tissues were obtained through the Experimental Animal Center of Wuhan University (Wuhan, China) using procedures approved by the Hubei Provincial Experimental Animal Quality Inspection Station for scientific research (permission license no.: SCXK2016-0009). Tissues were harvested from the abdomen of pigs (approximately 4.5 months old) immediately after euthanasia and included skin and underlying subcutis and muscle (35 mm). The tissue was trimmed, immediately vacuum sealed, and stored at -80 °C. Prior to injection, each sample was thawed at 22 °C and equilibrated to room temperature.

2.2 Injection experiments

In the injection experiments, a needle-free injector (INJEX 30 Pharma Gmbh, Berlin, Germany) was used in both the gel injection experiments and porcine injection experiments. Based on the supplied nozzle with a diameter of 0.17 mm, nozzles of other sizes were manufactured by a micro porous laser. The orifice diameter ranged from 0.17 mm to 0.50 mm, and the injected volume ranged from 0 mL to 0.35 mL. The single-variable method was conducted in both gel injection and porcine tissue injection. Thus, the orifice diameter was always 0.17 mm when the ejection volume changed from 0.05 mL to 0.35 mL. Similarly, as the diameter varied from 0.17 mm to 0.50 mm, the ejection volume maintained a value of 0.30 mL.

Five injections were performed at each data point in the injection experiments. Any fluid remaining on the surface of the gel or tissue following the injection was removed prior to weighing with a piece of tissue paper. The average value of the five injections of experimental data was used to analyze the experimental phenomenon. Moreover, an early pre-experiment found that the standoff distance has little influence on the stagnation pressure of the liquid jet when it was within 7 mm. Therefore, the value of the standoff distance in all injection experiments was 1 mm or less.

As for the impact experiments, an impact force measurement platform was used that was described in the previous research [25]. The platform contains a dynamic pressure sensor, an HBM data acquisition system (Quantum MX840B-8) and a desktop computer (Air14, Lenovo, China). When the jet impinges on the sensor, the data acquisition system acquires the signal change from the sensor. Then, the data acquisition system processes the acquired signal into an image signal using an internal processing program and displays it on the computer. In this study, the dynamic pressure sensor was replaced by a new model (M5156-000002-030BG) with the aim of capturing minute changes in the impact force.

The orifice average impact pressure can be converted according to the Bernoulli equation, as below:

$$P = \frac{\rho_0 v^2}{2} = \frac{F}{2A_0} \tag{1}$$

where P is the orifice average impact pressure, ρ_0 is the liquid density, v is the fluid velocity, F is the impact force on the sensor, and A_0 is the sectional area of the nozzle.

In addition, to depict the dispersion pattern of the liquid jet, the conventional parameters related to the liquid dispersion in the gel injection and porcine injection were obtained quantitatively, including L_c, the total depth of the dispersion, L_m, the distance from the surface corresponding to the maximum width of the dispersion region, L_s, the distance of the injection region, W_k, the maximum the width of the dispersion region, and W_c, the width of the injection region.

2.3 Mathematical model

As described by Schramm-Baxter and Mitragotri, the gel dispersion pattern is related to the jet power at the nozzle exit [26]:

$$E_0 = \frac{1}{8}\pi\rho D_0^2 v_0^3 \tag{2}$$

where E_0 is the jet power at the nozzle exit, ρ is the liquid density, D_0 is the orifice diameter of the injector and v_0 is the average velocity at the nozzle exit.

The average velocity at the nozzle exit can be calculated by the equation associated with the ejection volume:

$$v_0 = \frac{Q}{A_0} = \frac{V}{A_0 T} \tag{3}$$

where Q is the volume flowrate, V is the ejection volume, A_0 is the area of the nozzle exit, and T is the injection duration.

Therefore, the jet power can be calculated by the ejection volume and orifice diameter as shown in Eq. (4).

$$E_0 = \frac{1}{8}\pi\rho D_0^2\left[\frac{V}{A_0 T}\right]^3 = 8\rho\frac{1}{\pi^2 T^3}\frac{V^3}{D_0^4} \tag{4}$$

Based on this equation of the jet power, using the experimental data from the gel injection and porcine tissue injection experiments with a nozzle diameter of 0.17 to 0.50 mm and an ejection volume of 0.05 to 0.35 mL, research on the relationship between the jet power and delivery percent of liquid was conducted.

3. Results and discussion

3.1 Impact experiments

Fig. 1 presents the pressure profile in the impact experiments process. To evaluate the effect of the standoff distance on the injection pressure and injection duration, studies were performed using standoff distances ranging from 0 mm to 7 mm. As shown in Fig. 1(a), the maximum pressure decreased with increasing standoff distance. This is because the energy

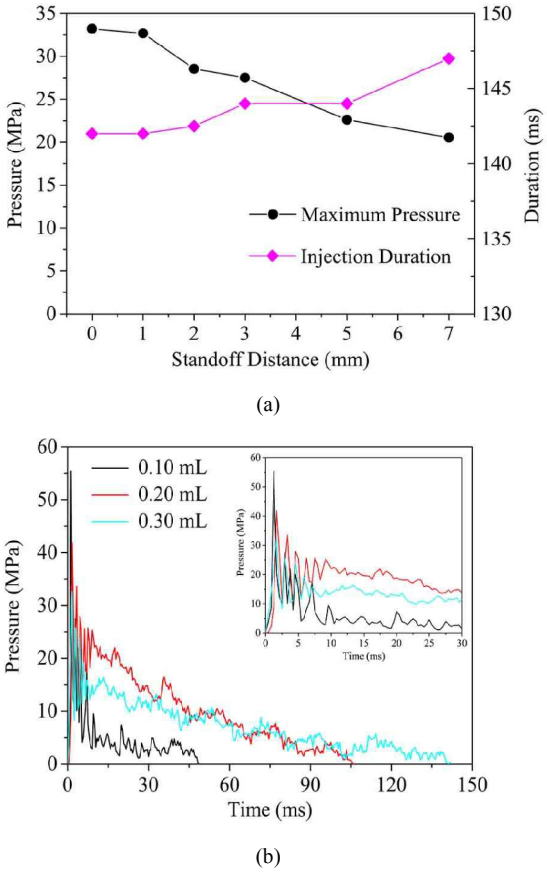

Fig. 1. (a) Diagram of the relationships between the injection maximum pressure/injection duration and the standoff distance; (b) experimental impact pressure for the entire injection process with ejection volumes of 0.10, 0.20, and 0.30 mL. The embedded figure shows impact pressures in the first 30 ms.

dissipation of the jet increases with increasing standoff distance. However, the maximum pressure was still over 15 MPa, which was generally able to penetrate into the epidermal layer and deliver the drug to the subcutaneous layer [27]. The injection duration varied between 142.5 ms and 147 ms, while the standoff distance was less than 7 mm. The total energy of the jet decreased with increasing standoff distance, causing a decrease in the kinetic energy of the jet according to the law of energy conservation. As a consequence, the duration of injection increases under the same ejection volume.

This means that the standoff distance influenced the NFI when it ranged from 0 mm to 7 mm. Therefore, the standoff distance in the following impact experiments was 1 mm or less. Furthermore, it could be concluded from Fig. 1(b) that the ejection volume had an important effect on the injection duration. When the ejection volume increased from 0.10 mL to 0.30 mL, the injection duration increased from 49 ms to 142 ms.

Fig. 2 shows the result of the pressure profile and injection duration obtained from the impact experiments with different ejection volumes and orifice diameters. For the injection pressure in Fig. 2(a), the pressure profile declined rapidly from

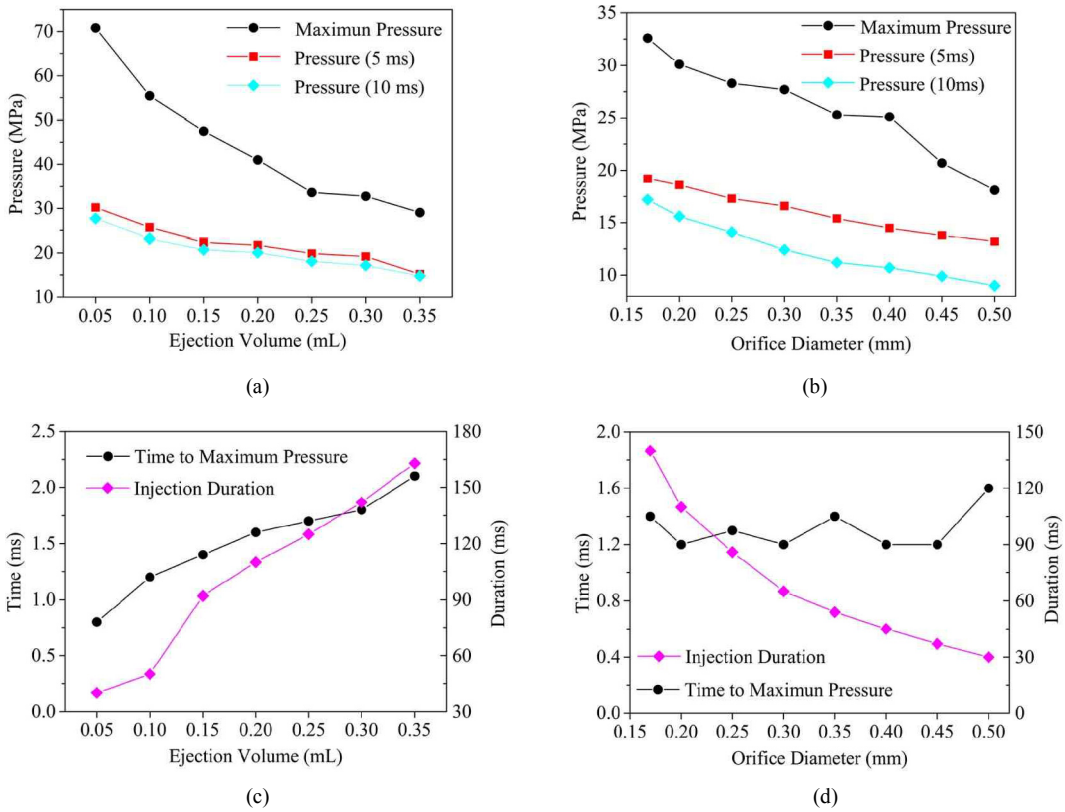

Fig. 2. Experimental impact pressure profile with (a) the ejection volume ranging from 0.05 mL to 0.35 mL; (b) the orifice diameter ranging from 0.17 mm to 0.50 mm; Diagram of the relationships between the injection duration/time to maximum pressure; (c) the different ejection volumes; (d) the different orifice diameters. The orifice diameter in (a) and (c) was 0.17 mm, and the ejection volume in (b) and (d) was 0.30 mL.

70.84 MPa to 29.04 MPa when the ejection volume increased from 0.05 mL to 0.35 mL, whereas the impact pressure in the first 5 ms and 10 ms after injection showed a slight change. According to the kinetic energy theorem, the instantaneous energy released by the spring is constant. As the ejection volume becomes larger, the kinetic energy of the liquids decreases, resulting in a decrease in the maximum pressure. Furthermore, it was indicated that the variation of the ejection volume affected the time to achieve the maximum pressure (see Fig. 2(c)). The time to reach the maximum pressure (2.10 ms) of the maximum ejection volume (0.35 mL) was approximately three times as much as with the minimum injection (0.72 ms, 0.05 mL). This phenomenon probably occurred because the greater the ejection volume, the greater the energy dissipation of the liquid is according to the Navier-Stokes equations and the law of energy conservation. Undoubtedly, the ejection volume played a significant role in the injection maximum pressure and injection duration.

In addition, the correlations between the injection maximum pressure profile and the orifice diameter of the injector are given in Fig. 2(b). The variation of the orifice diameter had an effect on the maximum pressure as well. The maximum pressure (32.60 MPa) of the injector with an orifice diameter of 0.17 mm was twice that of the injector (18.10 MPa) with an orifice diameter of 0.50 mm. The injection pressure in the first 5 ms and 10 ms after injection presented a linear decrease with increasing diameter. However, as can be seen in Fig. 2(d), the time to reach the maximum value maintained an average value of 1.30 ms and oscillated at a magnitude of 0.10 ms. The injection duration shortened from 140 ms to 30 ms with increasing orifice diameter, which was due to the increase of the mass flow rate according to hydrodynamic mass conservation. Thus, the orifice diameter of the injector has an effect on the injection pressure and duration.

3.2 Gel injection experiments

Fig. 3 shows the typical shape of jet penetration and dispersion into gels; the ejection volumes from left to right were 0.10 mL, 0.20 mL, and 0.30 mL. It was apparent that the area of the dispersion area became larger with increasing ejection volume, as shown in Fig. 3(a). In addition, the general measured parameters for the gels after injection are depicted in Fig. 3(b).

The quantitative measurement results of the dispersion characteristics in gel injection are described in Fig. 4. As shown in Fig. 4(a), the total depth of dispersion (L_c) and the maximum width of dispersion region (W_k) increased with increasing ejection volume. In particular, the value of L_c showed a sharp increase when the ejection volume increased from 0.20 mL to 0.25 mL, meaning that the area of the dispersion region increased by 50 % once the ejection volume ex-

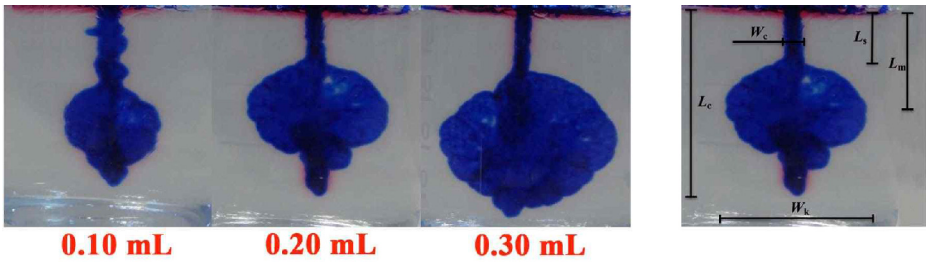

(a) (b)

Fig. 3. Experimental images for gel injection: (a) Front views of gels after NFI from jets with various ejection volumes; (b) processed images of the gel injection used to quantitatively measure the magnitude of the dispersion. L_c, the total depth of the dispersion; L_m, the distance from the surface to the location of the maximum width of the dispersion region; L_s, the distance of the injection region; W_k, the maximum width of the dispersion region; W_c, the width of the injection region. The orifice diameter in (a) was 0.17 mm.

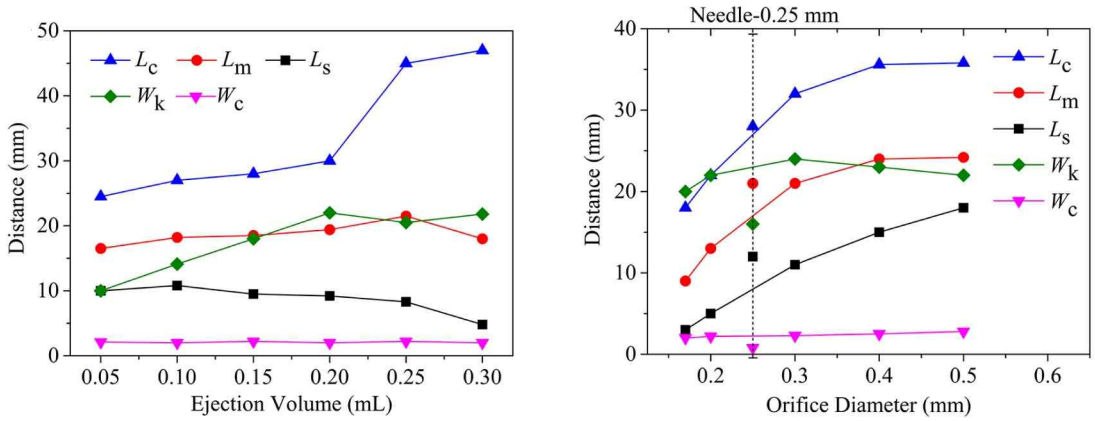

(a) (b)

Fig. 4. Characteristics of parameters related to the dispersion pattern in the gel injection: (a) The correlation between dispersion characteristics and the ejection volume; (b) the correlation between dispersion characteristics and the orifice diameter (the diameter of the needle in the needle injection was 0.25 mm). The orifice diameter in the (a) was 0.17 mm and the ejection volume in the (b) was 0.30 m.

ceeded 0.20 mL. In addition, there were no obvious changes in the distance from the surface corresponding to the maximum width of the dispersion region (L_m) and the width of the injection region (W_c) as the ejection volume changed. Instead, the distance of the injection region (L_s) decreased from 9.6 mm to 4.6 mm as the ejection volume increased from 0.05 mL to 0.30 mL. This was because the distance of the injection region became shorter with increasing ejection volume. Thus, it was clear that the ejection volume affected the width of the dispersion region during the gel injection.

Similarly, the effect of the orifice diameter on jet penetration into the gels is described in Fig. 4(b). The values of L_c, L_m and L_s all increased with increasing orifice diameter, while the values of W_k and W_c both showed little change, remaining nearly 2.5 mm and 22 mm, respectively. Consequently, it was indicated that the orifice diameter of the needle-free injector had a large effect on the length of the injection zone in the gel injection. Compared to the case of NFI, the values of L_c and W_c of the needle injection (with a needle diameter of 0.25 mm) exhibited a similar trend consistent with that of NFI. However, the values of L_s and W_k of the needle injection do not match the variation tendency of those in NFI. We are aware that L_s was controlled by the pressing force of the operators. The value of the W_k of the needle injection was certainly lower than that of NFI, which was because the needle-free injector had a better diffusion performance than that of needle injection. Overall, the ejection volume had a great influence on the width of the dispersion pattern, and the orifice diameter influenced the length of the diffusion region in the gel injection.

3.3 Porcine tissue injection experiments

The cross-sectional views of post-mortem porcine tissue after NFI from jets with different ejection volumes and orifice diameters are shown in Fig. 5. The ejection volumes from left to right are 0.10 mL, 0.20 mL, and 0.30 mL in Fig. 5(a), while the orifice diameters in Fig. 5(b) are 0.20 mm, 0.30 mm, 0.40 mm, and 0.50mm. As the injected volume increased, the area of the dispersion region and the fraction of fluid delivered beyond the dermis both increased. The explicit measurement results of liquid penetration into post-mortem porcine tissue are described in Fig. 6.

It can be observed from Fig. 6(a) that there were almost no changes in the values of the L_c and L_m with the variation of the

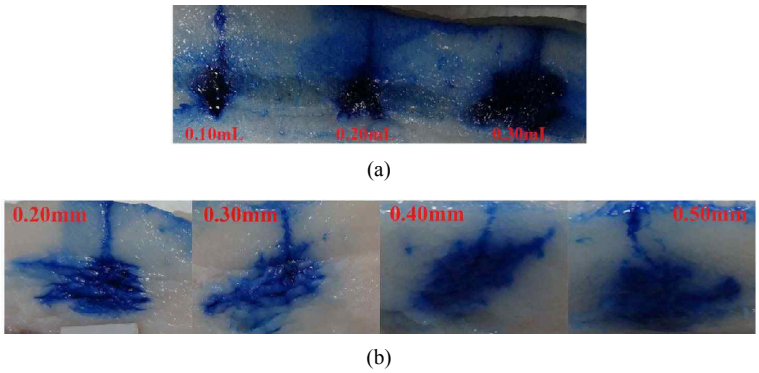

Fig. 5. Cross-sectional views of post-mortem porcine tissue after NFI from jets with (a) ejection volumes of 0.10 mL, 0.20 mL and 0.30 mL; (b) orifice diameters of 0.20 mm, 0.30 mm, 0.40 mm and 0.50 mm. The orifice diameter in the (a) was 0.17 mm and the ejection volume in the (b) was 0.30 mL.

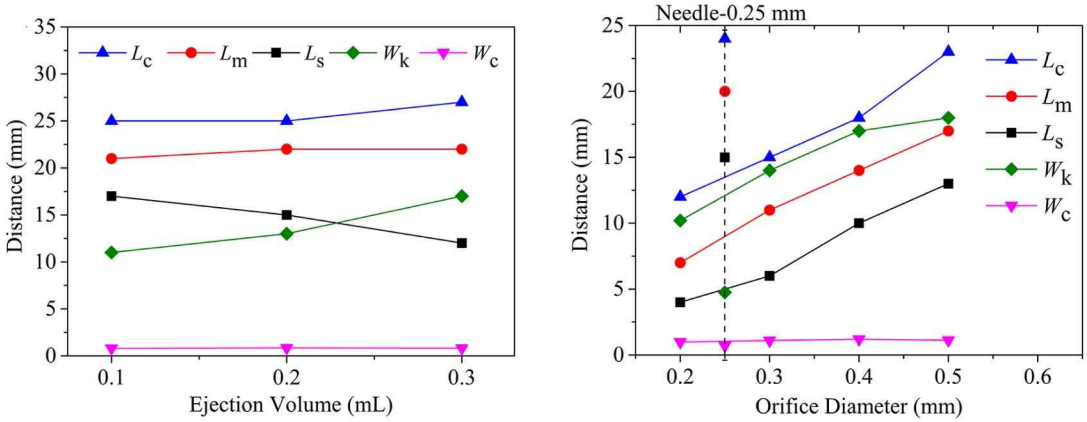

Fig. 6. Characteristics of parameters related to the dispersion pattern in the post-mortem porcine tissue injection: (a) The correlation between dispersion characteristics and the ejection volume; (b) the correlation between dispersion characteristics and the orifice diameter (the diameter of the needle in the needle injection was 0.25 mm). The orifice diameter in the (a) was 0.17 mm and the ejection volume in the (b) was 0.30 mL.

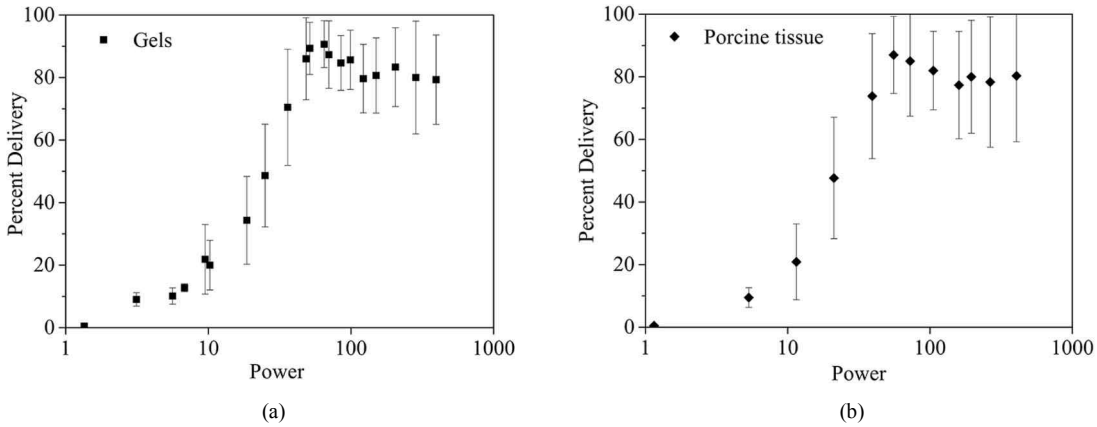

Fig. 7. The relationship between jet power and percent of fluid delivered into gels (a); porcine tissue (b) by jet injection on jet power. Error bars represent the standard deviation of five injections.

ejection volume. This phenomenon was similar to that observed in the gel injection, in which the length of the dispersion area remained unchanged with increasing ejection volume. The distance of the injection region showed a slight decreasing trend with increasing ejection volume. Nevertheless, as the ejection volume increased from 0.10 mL to 0.30 mL, the maximum width of the dispersion region increased from 11 mm to 17 mm, whose change rate exceeded 50 %. In addition, the width of the injection region was close to 0.82 mm. These results revealed that the ejection volume had an impor-

tant impact on the width of the dispersion area rather than the length of it.

Moreover, as can be seen from Fig. 6(b), the value of the parameters about the width of the dispersion area including L_c, L_m and L_s increased sharply with increasing orifice diameter. The value of L_c increased from 12 mm to 23 mm as the ejection volume increased from 0.20 mm to 0.50 mm. Additionally, the value of L_m presented the same trend, and the value (17 mm) of L_m in the injector with an orifice diameter of 0.50 mm was twice its value (7 mm) in the injector with an orifice diameter of 0.20 mm. This phenomenon was in accordance with the research that showed that the ejection volume varied the dispersion pattern [28]. In contrast, the width of the dispersion area showed slight variation. Therefore, a conclusion consistent with gel injection can be obtained that the variation of the ejection volume affects the width of the dispersion pattern; in addition, the orifice diameter plays a significant role in the length of the diffusion region in the post-mortem porcine tissue injection.

Additionally, the quantitative delivery percentages of liquid penetrate into gels and porcine tissues are shown in Fig. 7. The figure illustrates the phenomenon that the percent delivery increased exponentially with increasing jet power. When the value of the jet power ranged from 50 W to 70 W, the percent delivery reached the maximum value of more than 90 % both in gel injection and in porcine tissue injection. Then, as the jet power continued to increase, the percent delivery tended to decrease slightly. This result was consistent with that of some previous studies, which identified that the jet velocity and the ejection volume influenced the delivery percent of liquid in NFI [29-31]. Thus, the jet power calculated by the orifice diameter and ejection volume reliably described the behavior of the delivery fraction in the actual injection.

4. Conclusions

Based on the impact experiments and injection experiments for the gels and porcine, this work has provided informative descriptions of jet injector characteristics and performance. The ejection volume directly affected the injection duration in both the impact experiments and injection experiments for the gels and porcine tissue. Moreover, it had an important effect on the maximum pressure and the time to reach the maximum pressure. In addition, the variation of the orifice diameter had an influence on the maximum pressure and injection duration, whereas it did not influence the time to reach the maximum pressure. Overall, it could be concluded that the ejection volume had a great influence on the width of the dispersion pattern and that the orifice diameter influences the length of the diffusion region. More remarkably, the mathematical model of the jet power calculated by the orifice diameter and ejection volume reliably described the performance of the delivery fraction in the actual injection. Finally, these results can be used to guide the selection of the injection parameters of spring-loaded NFI for better injection efficiency and a satisfactory injection experience.

Conflicts of interest

The authors have no financial or non-financial interests that represent potential conflicts of interest.

Acknowledgements

This work was supported by the National Key Basic Research Program of China (grant number: 2014CB239203); the National Natural Science Foundation of China (NSFC) (grant number: 51474158); and the Natural Science Foundation of Hubei Province of China (Key Program) (grant number: 2016CFA088).

Nomenclature

NFI : Needle-free injection
A_0 : The area of the nozzle exit section
D_0 : Orifice diameter
E_0 : Jet power at the nozzle exit
L_c : The total depth of the dispersion
L_m : The distance from the surface to the location of maximum width of the dispersion region
L_s : The distance of the injection region
W_k : The maximum width of the dispersion region
W_c : The width of the injection region
Q : Volume flowrate
T : Injection duration
v_0 : Average velocity
ρ : Liquid density

References

[1] K. An, Y. S. Kim, H. Y. Kim, H. Lee, D. H. Hahm, K. S. Lee and S. K. Kang, Needle-free acupuncture benefits both patients and clinicians, *Neurological Research*, 32 (2010) S22-S26.

[2] S. Mitragotri, Current status and future prospects of needle-free liquid jet injectors, *Nature Reviews Drug Discovery*, 5 (7) (2006) 543-548.

[3] A. Arora, M. R. Prausnitz and S. Mitragotri, Micro-scale devices for transdermal drug delivery, *International Journal of Pharmaceutics*, 364 (2) (2008) 227-236.

[4] S. Mitragotri, Devices for overcoming biological barriers, The use of physical forces to disrupt the barriers, *Advanced Drug Delivery Reviews*, 65 (1) (2013) 100-103.

[5] R. Portaro and H. D. Ng, Experiments and modeling of air-powered needle-free liquid injectors, *Journal of Medical and Biological Engineering,* 35 (5) (2015) 685-695.

[6] A. Taberner, N. C. Hogan and I. W. Hunter, Needle-free jet injection using real-time controlled linear Lorentz-force actuators, *Medical Engineering and Physics,* 34 (9) (2012) 1228-1235.

[7] A. J. Taberner, N. B. Ball, N. C. Hogan and I. W. Hunter, A portable needle-free jet injector based on a custom high power-density voice-coil actuator, *28th Annual International Conference of the IEEE Engineering in Medicine and*

Biology Society, 1-15 (2006) 2531-2534.
[8] J. C. Stachowiak, M. G. von Muhlen, T. H. Li, L. Jalilian, S. H. Parekh and D. A. Fletcher, Piezoelectric control of needle-free transdermal drug delivery, *Journal of Controlled Release,* 124 (1-2) (2007) 88-97.
[9] S. Mitragotri, Immunization without needles, *Nature Reviews Immunology,* 5 (12) (2005) 905-916.
[10] D. L. Bremseth and F. Pass, Delivery of insulin by jet injection: recent observations, *Diabetes Technology and Therapeutics*, 3 (2) (2001) 225.
[11] A. Mohizin and J. K. Kim, Current engineering and clinical aspects of needle-free injectors: A review, *Journal of Mechanical Science and Technology,* 32 (12) (2018) 5737-5747.
[12] A. B. Baker and J. E. Sanders, Fluid mechanics analysis of a spring-loaded jet injector, *IEEE Transactions on Biomedical Engineering*, 46 (2) (1999) 235-242.
[13] G. Park, A. Modak, N. C. Hogan and I. W. Hunter, The effect of jet shape on jet injection, *Proceedings of Annual International Conference of the IEEE Engineering in Medicine and Biology Society IEEE Engineering in Medicine and Biology Society Annual Conference,* 2015 (2015) 7350-7353.
[14] A. Schoubben, A. Cavicchi, L. Barberini, A. Faraon, M. Berti, M. Ricci, P. Blasi and L. Postrioti, Dynamic behavior of a spring-powered micronozzle needle-free injector, *International Journal of Pharmaceutics*, 491 (1-2) (2015) 91-98.
[15] J.-I. Imoto, T. Ishikawa, A. Yamanaka, M. Konishi, K. Murakami, T. Shibahara, M. Kubo, C.-K. Lim, M. Hamano, T. Takasaki, I. Kurane, H. Udagawa, Y. Mukuta and E. Konishi, Needle-free jet injection of small doses of Japanese encephalitis DNA and inactivated vaccine mixture induces neutralizing antibodies in miniature pigs and protects against fetal death and mummification in pregnant sows, *Vaccine,* 28 (46) (2010) 7373-7380.
[16] J. C. Stachowiak, T. H. Li, A. Arora, S. Mitragotri and D. A. Fletcher, Dynamic control of needle-free jet injection, *Journal of Controlled Release*, 135 (2) (2009) 104-112.
[17] M. Moradiafrapoli and J. O. Marston, High-speed video investigation of jet dynamics from narrow orifices for needle-free injection, *Chemical Engineering Research and Design*, 117 (2017) 110-121.
[18] G. Zhang, I. I. Lee, T. Hashimoto, T. Setoguchi and H. D. Kim, Experimental studies on shock wave and particle dynamics in a needle-free drug delivery device, *Journal of Drug Delivery Science and Technology,* 41 (2017) 390-400.
[19] J. Baxter and S. Mitragotri, Jet-induced skin puncture and its impact on needle-free jet injections: Experimental studies and a predictive model, *Journal of Controlled Release,* 106 (3) (2005) 361-373.
[20] J. Schramm-Baxter, J. Katrencik and S. Mitragotri, Jet injection into polyacrylamide gels: Investigation of jet injection mechanics, *Journal of Biomechanics*, 37 (8) (2004) 1181-1188.
[21] J. H. Chang, N. C. Hogan and I. W. Hunter, A needle-free technique for interstitial fluid sample acquisition using a lorentz-force actuated jet injector, *Journal of Controlled Release,* 211 (2015) 37-43.
[22] K. Comley and N. Fleck, Deep penetration and liquid injection into adipose tissue, *Journal of Mechanics of Materials and Structures,* 6 (1-4) (2011) 127-140.
[23] T. P. Sullivan, W. H. Eaglstein, S. C. Davis and P. Mertz, The pig as a model for human wound healing, *Wound Repair and Regeneration,* 9 (2) (2001) 66-76.
[24] J. Schramm and S. Mitragotri, Transdermal drug delivery by jet injectors: Energetics of jet formation and penetration, *Pharmaceutical Research,* 19 (11) (2002) 1673-1679.
[25] D. P. Zeng, Y. Kang, L. Xie, X. X. Xia, Z. F. Wang and W. C. Liu, A mathematical model and experimental verification of optimal nozzle diameter in needle-free injection, *Journal of Pharmaceutical Sciences,* 107 (4) (2018) 1086-1094.
[26] J. Schramm-Baxter and S. Mitragotri, Needle-free jet injections: Dependence of jet penetration and dispersion in the skin on jet power, *Journal of Controlled Release*, 97 (3) (2004) 527-535.
[27] O. A. Shergold, N. A. Fleck and T. S. King, The penetration of a soft solid by a liquid jet, with application to the administration of a needle-free injection, *Journal of Biomechanics*, 39 (14) (2006) 2593-2602.
[28] T. M. Grant, K. D. Stockwell, J. B. Morrison and D. D. Mann, Effect of injection pressure and fluid volume and density on the jet dispersion pattern of needle-free injection devices, *Biosystems Engineering*, 138 (2015) 59-64.
[29] W. Seehanam, K. Pianthong, W. Sittiwong and B. Milton, Injection pressure and velocity of impact-driven liquid jets, *Engineering Computations*, 31 (7) (2014) 1130-1150.
[30] R. M. J. Williams, B. P. Ruddy, N. C. Hogan, I. W. Hunter, P. M. F. Nielsen and A. J. Taberner, Analysis of moving-coil actuator jet injectors for viscous fluids, *IEEE Transactions on Biomedical Engineering*, 63 (6) (2016) 1099-1106.
[31] J. W. McKeage, B. P. Ruddy, P. M. F. Nielsen and A. J. Taberner, The effect of jet speed on large volume jet injection, *Journal of Controlled Release*, 280 (2018) 51-57.

Dongping Zeng received his B.S. degree from Northwest Agriculture Forestry University, Xian, China, in 2016 and is now a Ph.D. candidate in the School of Power and Mechanical Engineering, Wuhan University, Wuhan, China. He focuses on the mechanical principles and clinical applications of needle-free jet injectors.

Yong Kang received his B.S. and Ph.D. degrees from Chongqing University, China, in 2001 and 2006, respectively. He is now a Professor and the Vice Dean of the School of Mechanical Engineering, Wuhan University, Wuhan, China. His research interests include biomedical engineering, water-jet technology and mining technology.